UNITED NATIONS UNIVERSITY
GEOTHERMAL TRAINING PROGRAMME
Orkustofnun, Grensasvegur 9,
IS-108 Reykjavik, Iceland

Reports 2011
Number 33

ANALYSIS OF WELL TEST DATA FOR THE ESTIMATION OF RESERVOIR PARAMETERS AND THE PREDICTION OF PRESSURE RESPONSE USING WELLTESTER AND LUMPFIT

Nazrul Islam Syed
Geological Survey of Bangladesh
153 Pioneer Road, Segunbagicha
Dhaka 1000
BANGLADESH
nazrulgsb@yahoo.com

ABSTRACT

This work presents a review of the theoretical background and methodology used in the analysis of well test data from four geothermal wells. The purpose of the well test analysis is to identify the type of reservoir involved and to quantitatively determine the reservoir parameters. The injection well test data of three wells were analysed using the software WellTester and one set of interference test data was analysed by the software Lumpfit. WellTester has been used extensively in Iceland for the estimation of reservoir properties whereas the Lumpfit has been used for future pressure response prediction for various production scenarios as well as to determine some reservoir properties. Important parameters such as transmissivity, permeability, and storativity for groundwater flow models were estimated in order to predict the future availability of the water resource. To determine these parameters and others, injection well test pressure response data from three wells at Hellisheidi high-temperature area were analysed. The well test analysis results show that the reservoir is generally characterized by good permeability and storativity. Generally, above average values of the injectivity index were also observed. The results for these parameters are in the normal range for Iceland.

The second part of the project included an analysis of an interference test at a low temperature field. The entire 232 days of monitoring of pressure response data, taken in one observation well, due to the production of two production wells was simulated by lumped parameter modelling. Modelling showed that different combinations of two- and three-tank closed and open models fit satisfactorily. The future water-level changes in the observation well were predicted, based on three production scenarios. The calculated results for open tank models indicated that this system would be able to sustain an average of 80 kg/s production for ten years without significant pressure drop.

1. INTRODUCTION

Iceland is located at the Mid-Atlantic Ridge, where the North-American and Eurasian plates spread apart. The spreading rate is on the average almost 2 cm/year in S-Iceland, according to GPS

measurements done in 1995 to 2010 (Geirsson et al., 2010). Iceland is predominantly composed of basaltic rock. Stratigraphically, Icelandic rock is divided into four groups: Tertiary (Mio-Pliocene), (older than 3.1 m.y.), Plio-Pleistocene (3.1-0.7 m.y.), Upper-Pleistocene (700,000-11,000 y.), Postglacial (11,000 y. and younger) (Fridleifsson, 1983). The exposed volcanic pile is built predominantly of basalt (80-85%) and acidic rock, including intermediate rocks which constitute about 10%. The amount of sediment of volcanic origin is on the order of 5-10% in a typical Tertiary lava pile but much higher in Quaternary rocks. Among the basalts, three main lava types have been recognized. They are olivine-tholeiite, tholeiite and porphyritic with plagioclase and/or pyroxene.

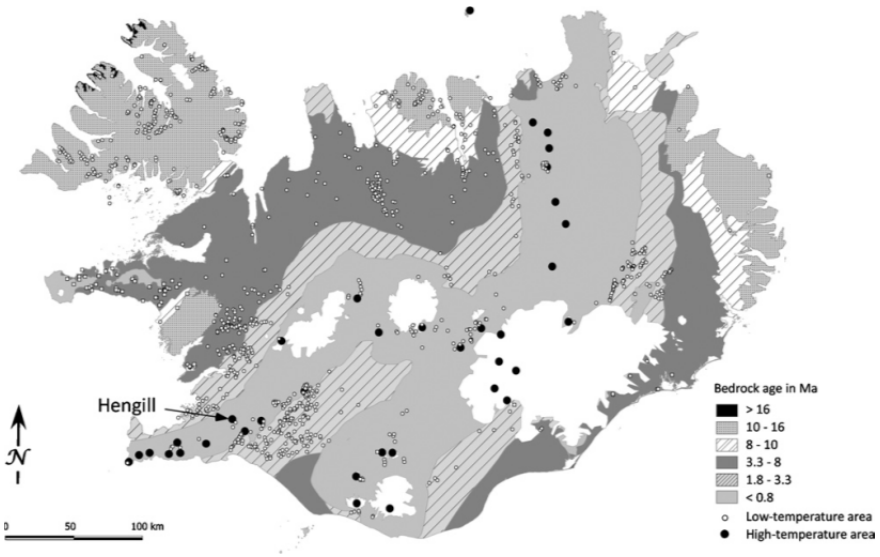

FIGURE 1: A geological and geothermal map of Iceland and the location of the Hengill volcano (from Árnason et al., 2010)

A neovolcanic zone crosses Iceland from southwest to northeast and has been divided into an axial rift zone and flank zones (Figure 1). The axial rift zone is under tensional stress parallel to the spreading direction. It is characterized by numerous volcanic systems which are composed of open fissures, grabens and crater rows of 10 km to over 100 km in length. All high-temperature geothermal fields are located in this zone. On the other hand, the flank zones are isolated volcanic zones off the main axial rift zone. They are characterized by transitional alkaline basalts and shear stress regimes (Saemundsson, 1978; Jakobsson, 1972). The low-temperature geothermal fields are spread over most parts of Iceland, while the larger ones are found in lowland regions flanking the volcanic rift zone.

The Hengill central volcano is located in the middle of the southwestern volcanic zone (Figure 1) about 25 km east of Reykjavik city. The area consists of a triple junction where two active rift zones, i.e. the Reykjanes Peninsula volcanic zone and the Western volcanic zone, meet a seismically active transform zone, the South Iceland seismic zone. Mt. Hengill consists mainly of hyaloclastite formations (formed sub-glacially) which mostly accumulate around the volcanic crater, with interglacial lava successions found between the eruptive materials from the glacial periods. Wells HE-41, HE-42 and HE-45 are located in Hellisheidi which is a part of the Hengill high-temperature field. It is situated in the southern sector of the Hengill central volcano, south of the Nesjavellir high-temperature field. Since 1985, about 57 production wells have been drilled in the Hellisheidi high-temperature area. Well HE-42 was drilled vertically while the other two are directional.

2. WELL TESTING

2.1 General

Well testing is a measurement of pressure as a function of time for different flow rates that are kept constant for a period of time and then suddenly changed, forming steps. The pressure data is analysed using a pressure transient analysis which is a powerful tool. Well testing is an important phase for

reservoir characterization and the development of any geothermal resource. Well tests are performed to acquire qualitative and quantitative knowledge of the well and the reservoir being tested. During a well test, the pressure response, which is one of the most important parameters involved in geothermal exploration, to changing production or injection is monitored. During production, the mass and heat transport forced upon the system causes spatial as well as transient changes in the pressure state of the reservoir.

The differential equation which is used in geothermal reservoir physics to evaluate the mass transfer in the models of geothermal reservoirs, as well as to estimate reservoir pressure changes, is the so called pressure diffusion equation. It is derived by combining the conservation of mass and Darcy's law for the mass flow which, in fact, replaces the force balance equation in fluid mechanics.

2.2 Theoretical background

2.2.1 The pressure diffusion equation

The pressure diffusion equation is derived using several simplifying assumptions: the reservoir is infinitely large, confined, homogeneous and isotropic; the flow is horizontal and isothermal; the reservoir is completely saturated with a single fluid; the well penetrates the entire formation thickness. The pressure (P) in the reservoir at a certain distance (r) from a production well producing at a given rate (q) as a function of time (t) is determined by the pressure diffusion equation. For deriving the pressure diffusion equation, the three governing laws used are as follows (Earlougher, 1977; Horne, 1995):

1. *Conservation of mass within a control volume:*

Mass entering an element – Mass leaving an element = Rate of change of mass inside the element (1)

2. *Conservation of momentum, expressed by Darcy's law:*

$$q = 2\pi r h \frac{k}{\mu}\frac{\partial P}{\partial r} \tag{2}$$

where q = Volumetric flow rate (m^3/s), $q>0$ for flow towards the well;
h = Reservoir thickness (m);
k = Formation permeability (m^2);
P = Reservoir pressure (Pa);
r = Radial distance (m);
μ = Dynamic viscosity of the fluid (Pa·s)

3. *The state of the fluid equation:*

$$\rho = \rho(P, T)$$

4. *The compressibility of the fluid equation*:

$$c_f = \frac{1}{\rho}\left(\frac{\partial \rho}{\partial P}\right)_T \tag{3}$$

where c_f = Compressibility of the fluid (Pa^{-1});
ρ = Density of the fluid (kg/m^3);
T = Temperature (°C);
P = Pressure (Pa).

Using the above assumptions and combining the three equations above, the pressure diffusion equation is given by:

$$\frac{1}{r}\frac{\partial}{\partial r}\left(\frac{r\partial P(r,t)}{\partial r}\right)=\frac{\mu c_t}{k}\frac{\partial P(r,t)}{\partial t}=\frac{S}{T}\frac{\partial P(r,t)}{\partial t} \tag{4}$$

where c_t $= \varphi c_f + (1-\varphi)c_r$;
φ = Porosity;
c_r $= \frac{1}{1-\varphi}\frac{\partial \varphi}{\partial p}$ = The compressibility of the porous rock (Pa^{-1});
S $= c_t h$ = The storativity (m/Pa); and
T $= \frac{kh}{\mu}$= The transmissivity (m^3/(Pa·s).

In 1935, Theis proposed an integral solution to this equation (Earlougher, 1977; Horne, 1995), using the following initial and boundary conditions:

Initial condition: $P(r, t) \rightarrow P_i$ for $t = 0$ and for all: $r > 0$

Boundary conditions:

i. $P(r, t) = P_i$ for $r \rightarrow \infty$ for all $t > 0$
ii. $q = \frac{2\pi kh}{\mu}\lim_{r\rightarrow 0}\left(r\frac{\partial P}{\partial r}\right)$ for all $t > 0$

The solution of the pressure diffusion equation for radial flow with the above boundary and initial conditions is given by:

$$P(r,t) = P_i + \frac{q\mu}{4\pi kh}E_i\left(\frac{-\mu c_t\, r^2}{4kt}\right) \tag{5}$$

where $Ei(-x) = -\int_x^{\infty}\frac{e^{-u}}{u}du$ is the exponential integral function.

For $t > 25\frac{\mu c_t\, r^2}{4k}$, the exponential integral function can be expanded by a convergent series. Thus, the Theis solution for a pumping well with skin gives, using this assumption, the total pressure change, at the wellbore with radius r_w, as:

$$\Delta P_t = P_i - P(r,t) = -\frac{2.203q\mu}{4\pi kh}\left[log\left(\frac{\mu c_t r_w^2}{4kt}\right)+\frac{0.5772-2s}{2.303}\right] \tag{6}$$

where s is the skin factor, but skin is an additional pressure change to the normal pressure change in the near vicinity of the well due to the effects of drilling the well. A negative skin factor indicates that the well is in good communication with the reservoir.

2.2.2 Semi-logarithmic well test analysis

In science and engineering, a semi-log graph or semi-log plot is a way of visualizing data that are changing with an exponential relationship. This kind of plot is useful when one of the variables being plotted covers a large range of values and the other has only a restricted range – the advantage being that it can bring out features in the data that would not easily be seen if both variables had been plotted linearly**.** The Theis solution without skin can be written as:

$$P_i - P(r,t) = \frac{2.303q\mu}{4\pi kh}\left[log\left(\frac{4k}{\mu c_t\, r^2}\right)-\frac{\gamma}{2.303}\right]+\frac{2.303q\mu}{4\pi kh}logt \tag{7}$$

where γ = 0.5772 is the Euler constant.

The above equation is in the form: $\Delta P = A + mlogt$, which is a straight line with slope m on a semi-log graph where m is the pressure change per one log-cycle and:

$$\Delta P = P_i - P(r,t)\ ; A = \frac{2.303q\mu}{4\pi kh}\left[log\left(\frac{4k}{\mu c_t\, r^2}\right) - \frac{\gamma}{2.303}\right]\ and\ m = \frac{2.303q\mu}{4\pi kh}$$

The formation transmissivity, T, can be calculated from the slope of the semi-log straight line by:

$$T = \frac{kh}{\mu} = \frac{2.303q}{4\pi m} \tag{8}$$

If the temperature is known, then the dynamic viscosity, μ can be inferred from steam tables and the permeability thickness, kh, may be calculated as follows:

$$kh = \frac{2.303q\mu}{4\pi m} \tag{9}$$

The formation storativity or storage coefficient, $S = c_t h$, is then obtained using the coordinates of some point $(t,\Delta P)$ on the semi-log straight line, when the permeability thickness and the initial pressure are known. The Theis solution can then be written as:

$$\frac{\Delta P}{m} = \left[log\left[\left(\frac{4kh}{\mu}\right)\left(\frac{1}{S}\right)\left(\frac{t}{r^2}\right)\right] - \frac{\gamma}{2.303}\right] = log\left(\frac{2.246T}{Sr^2}t\right) \tag{10}$$

or

$$10^{\frac{\Delta p}{m}} = \left(\frac{kh}{\mu}\right)\left(\frac{1}{S}\right)\left(\frac{t}{r^2}\right)(2.246) = \frac{2.246T}{Sr^2}t$$

The storativity can be obtained by:

$$S = 2.246\left(\frac{kh}{\mu}\right)\left(\frac{t}{r^2}\right) \times 10^{-\frac{\Delta P}{m}} \tag{11}$$

Since, the transmissivity , $T = kh/\mu$, then:

$$S = 2.246T\left(\frac{t}{r^2}\right) \times 10^{-\frac{\Delta P}{m}} \tag{12}$$

When a well is opened to flow or shut in for a build-up, the rate of change at the surface is not instantaneously transmitted to the surface. The actual rate at which the change is transmitted to the surface is a function of the distance to the surface and the compressibility of the medium through which it travels. As a result, there is a gradual change in the rate to the desired value. This phenomenon is called wellbore storage or after flow. This flow regime occurs immediately following the shutting in or opening of the well. Wellbore storage effects can be caused in several ways, but there are two common means. One is storage by fluid expansion; the other is storage by changing the liquid/water level (Horne, 1995).

The wellbore storage coefficient, C [m^3/Pa] is a parameter used to quantify the effect; ΔV is the volume of fluid that the wellbore itself will produce due to a unit drop in pressure of ΔP:

$$C = \frac{\Delta V}{\Delta P} \tag{13}$$

With $\Delta V = Qt$, this becomes:

$$\Delta P = \frac{Q}{C}.t \quad or \quad \log(\Delta P) = \log(t) + log\frac{Q}{C}$$

So, wellbore storage is identified as a unit slope line on a log (ΔP) vs. log (t) graph. After about 1½ log cycle from the time when the pressure response starts to deviate from the unit slope line, the semi log straight line, representing the Theis solution, is expected to start.

Pressure transmission does not take place uniformly throughout the reservoir since it is affected by local heterogeneities. For the most part, these do not affect the pressure change within the well, except for those reservoir heterogeneities that are in the immediate vicinity of the wellbore. In particular, there is often a zone surrounding the well which is invaded by mud filtrate or cement during the drilling or completion of the well. This zone is called the skin zone; see Figure 2. It produces an additional pressure drop, ΔP_s near the wellbore to the normal reservoir pressure change due to production.

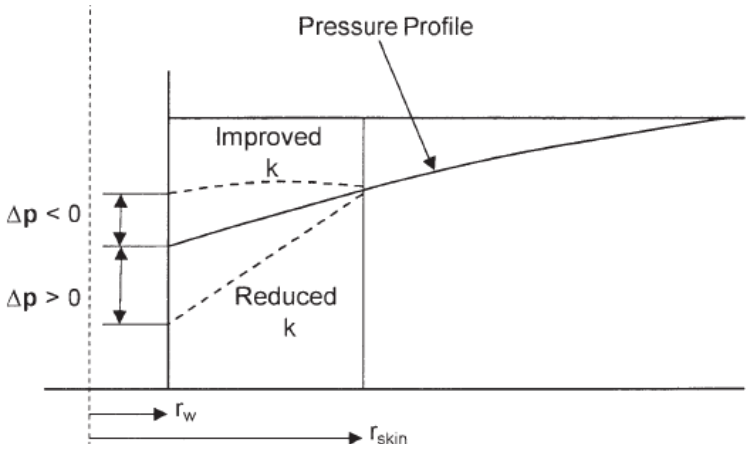

FIGURE 2: Representation of positive and negative skin effect

$$\Delta P_s = \frac{q\mu}{2\pi kh} \cdot s \tag{14}$$

where s = skin factor (dimensionless).

If we imagine that the skin effect is due to a damaged zone of radius r_s and reduced permeability, k_s then the skin factor can be calculated from:

$$s = \left(\frac{k}{k_s} - 1\right) ln\left(\frac{r_s}{r_w}\right) \tag{15}$$

Equation 15 provides some insight into the physical significance of the sign of the skin factor. There are only three possible outcomes in evaluating the skin factor:

- Positive skin factor ($s > 0$), when a damaged zone near the wellbore exists, k_s is less than k and hence s is a positive number. The magnitude of the skin factor increases as k_s decreases and as the depth of the damage r_s increases.
- Negative skin factor ($s < 0$), when the permeability around the well k_s is higher than that of the formation k, a negative skin factor exists. This negative factor indicates an improved wellbore condition.
- Zero skin factor ($s = 0$), occurs when no alteration in the permeability around the wellbore is observed, i.e. $k_s = k$.

In semi-log analysis, the skin factor does not affect the evaluation of transmissivity but it does affect the evaluation of storativity as shown in the following equation:

$$c_t h e^{-2s} = 2.246\left(\frac{kh}{\mu}\right)\left(\frac{t}{{r_w}^2}\right) \times 10^{-\frac{\Delta P}{m}} \tag{16}$$

3. INJECTION TEST DATA ANALYSIS AND ITS INTERPRETATION

An injection test, which is usually performed in high-temperature wells at the end of drilling, is preformed when water is injected into the well and the pressure response is recorded at a certain depth in the well. Well test injection data from three wells, HE-41, HE-42 and HE-45, at Hellisheidi, were analysed with the software WellTester (Júlíusson, et al., 2008). Most of the following text was generated by the WellTester report. The initial parameter values used for the analysis of the wells are summarized in Table 1.

TABLE 1: Initial parameters of various wells used in WellTester

Name of parameter and unit	Well		
	HE-41	HE-42	HE-45
Estimated reservoir temperature [°C]	260	286	280
Estimated reservoir pressure [bar-g]	135	147	132
Wellbore radius, r, [m]	0.16	0.16	0.16
Dynamic viscosity of reservoir fluid, μ, [Pa·s]	10.4×10^{-5}	9.38×10^{-5}	9.57×10^{-5}
Total compressibility, c_t, [Pa^{-1}]	1.69×10^{-10}	2.3×10^{-10}	2.17×10^{-10}
Porosity, φ	0.1	0.1	0.1
Compressibility of water, c_w, [Pa^{-1}]	1.47×10^{-9}	2.08×10^{-9}	1.95×10^{-9}
Compressibility of rock, c_r, [Pa^{-1}]	2.44×10^{-11}	2.44×10^{-11}	2.44×10^{-11}

3.1 Well HE-41

A three steps injection test was conducted in the directional well HE-41 on March 3, 2008 and lasted about 9 hours. The pressure gauge was placed at 1,750 m depth to monitor the pressure changes in the well. Total depth of the well was 2,843 m, the casing was placed at 781.5 m depth and KOP was at 320 m. The three step injection rates were 40, 60 and 25 L/s, respectively (Figure 3), with an initial rate of 25 L/s. The pressure response curves of the injection steps were very distinct. Each step of the pressure response curve was analysed. Using a trial and error method, various models were checked, after which the best model for all steps was selected; this is summarized in Table 2.

TABLE 2: Summary of the model selected for the well test analysis of well HE-41

Reservoir	Homogeneous
Boundary	Constant pressure
Well	Constantskin
Wellbore	Wellbore storage

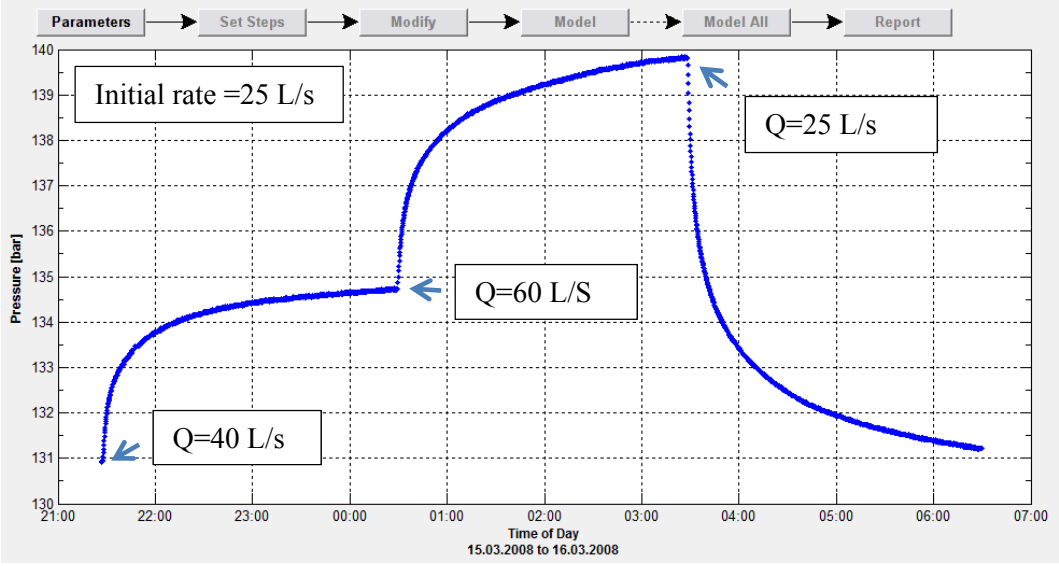

FIGURE 3: Pressure against time at 1750 m depth in well HE-41 during an injection test

3.1.1 Modelling of step 1, HE-41

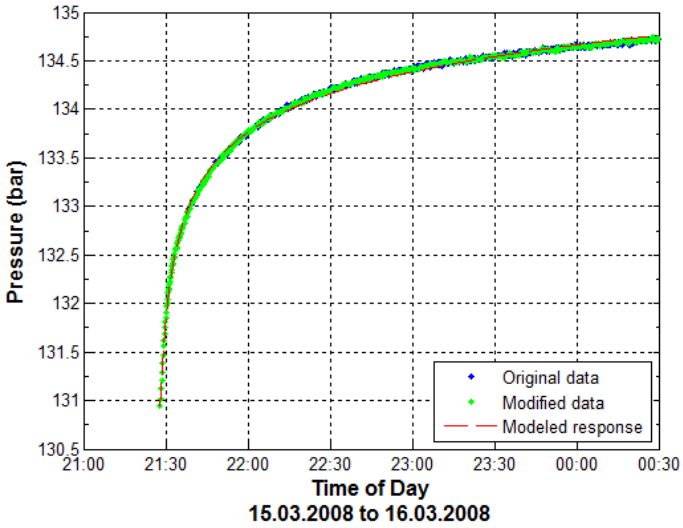

FIGURE 4: Fit between the model and original data for step 1 of well HE-41

A nonlinear regression analysis was performed to find the model parameters that best fit the data collected. The results from the regression analysis are shown graphically in Figure 4. Figure 5 shows the same data on a log-linear scale (left) and log-log scale (right). The plot on the log-log scale also shows the derivative of the pressure response, multiplied by the time passed since the beginning of the step. Derivative plots are helpful in determining the most appropriate model for the reservoir studied. The model fits the data fairly well and can be taken as representative of the reservoir response for step no. 1. Based on this model, different reservoir parameters were calculated and the results are presented in Table 3.

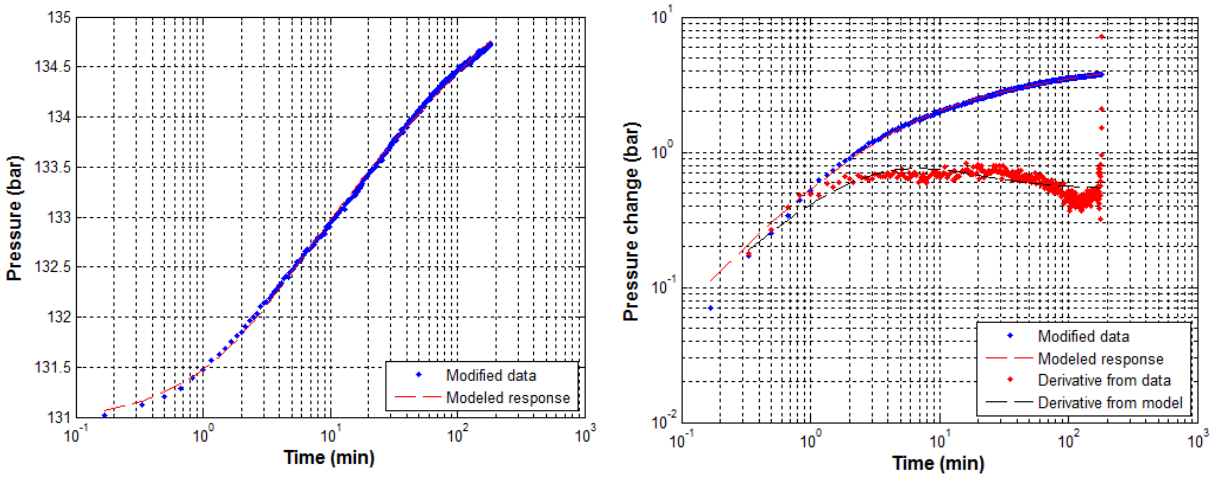

FIGURE 5: Pressure against time showing the fit between the model and the selected data of step 1 on a log-linear scale (left) and a log-log scale (right), HE-41

TABLE 3: Summary of results from non-linear regression parameter estimates for step 1, step 2, step 3 and all steps jointly, for well HE-41

Parameter name and unit	Step 1		Step 2		Step 3		All steps	
	Values	C_v%	Values	C_v%	Values	C_v%	Values	C_v%
Transmissivity (T) [(m^3/Pa·s)]	1.99×10^{-8}	0.58	1.75×10^{-8}	0.22	2.27×10^{-8}	0.29	2.01×10^{-8}	0.69
Storativity (S) [m^3/(Pa·m^2)]	5.01×10^{-8}	2.10	4.79×10^{-8}	1.21	4.52×10^{-8}	1.36	4.94×10^{-8}	2.19
Radius of investigation (r_e) [m]	90	1.51	127	1.42	115	1.04	99	1.43
Well skin	-3.14		-3.54		-2.95		-3.2	
Wellbore storage (C) [m^3/Pa]	9.53×10^{-6}	9.76	8.29×10^{-6}	8.51	1.1×10^{-5}	0.63	9.4×10^{-6}	2.44
Injectivity index (II) [(L/s)/bar]	4		3.91		4		4	
Reservoir thickness [m]	300		280		270		290	
Permeability (k) [m^2]	6.99×10^{-15} (7 mD)		6.41×10^{-15} (6.4 mD)		8.8×10^{-15} (8.8 mD)		7.13×10^{-15} (7.1 mD)	

3.1.2 Modelling of step 2, HE-41

The results from the regression analysis of step 2 are shown graphically in Figure 6 and the same results are shown graphically on a log-linear as well as a log-log scale in Figure 7. The model corresponds quite well with the pressure response of reservoir. Results for this step are shown in Table 3.

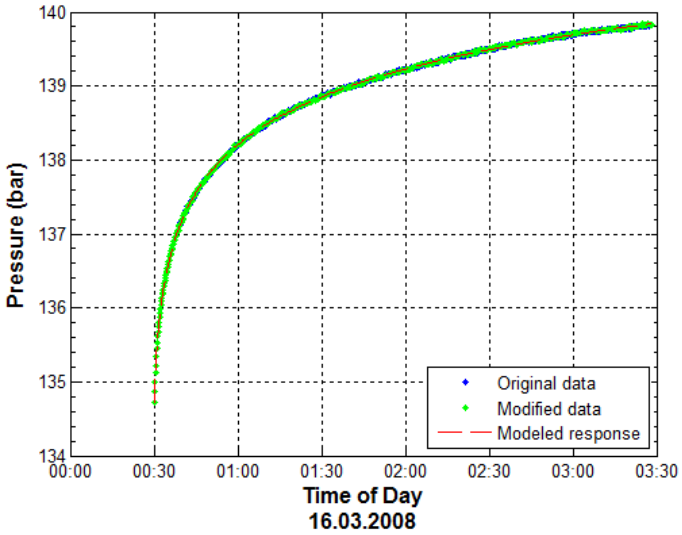

FIGURE 6: Fit between the model and original data for step 2 of well HE-41

3.1.3 Modelling of step 3, HE-41

The results from the regression analysis of step 3 are shown graphically in Figure 8 and the same results are shown graphically on a log-linear as well as a log-log scale in Figure 9. The model corresponds quite well with the pressure response of the reservoir. Results for this step are shown in Table 3.

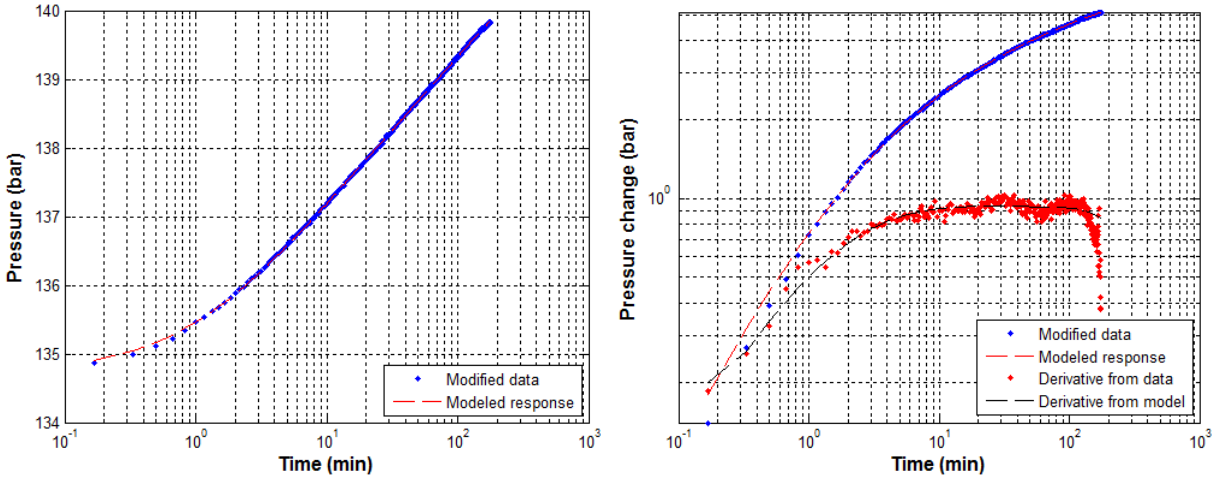

FIGURE 7: Pressure against time showing the fit between the model and the selected data of step 2 on a log-linear scale (left) and a log-log scale (right), HE-41

3.1.4 Modelling of all steps, HE-41

The three steps were modelled together starting with steps 1-3. The results from the regression analysis of the all step model are shown in Figure 10. The graph shows that the model from step 1 fits best. The results are presented in Table 3.

From Table 3 it can be seen that the transmissivity and storativity values are very consistent and that the values did not change very much throughout all the steps.

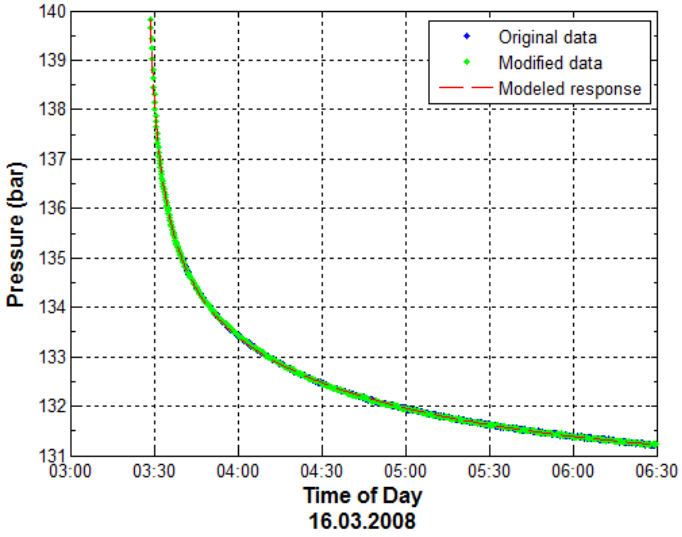

FIGURE 8: Fit between the model and original data for step 3 of well HE-41

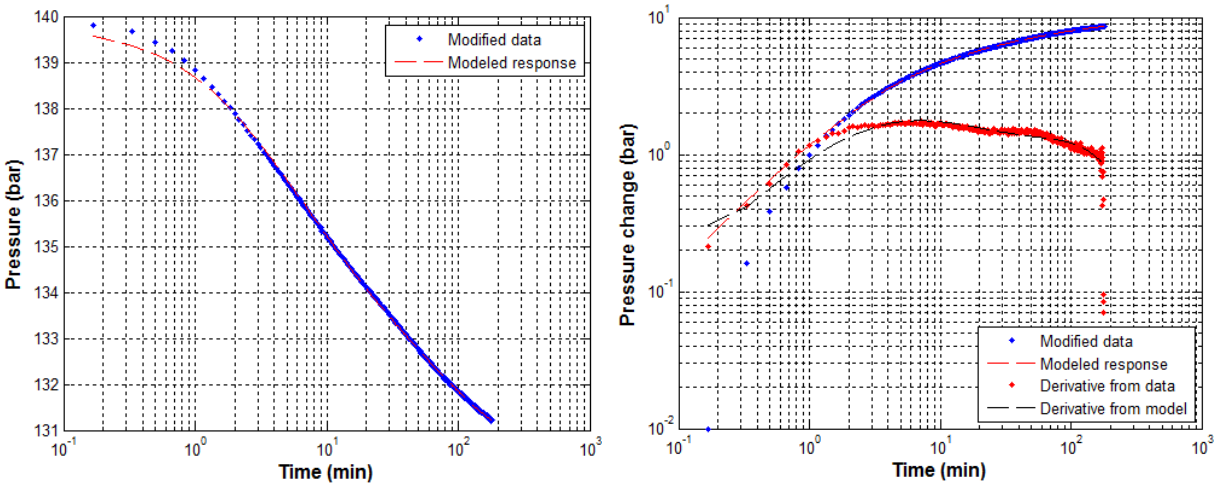

FIGURE 9: Pressure against time showing the fit between the model and the selected data of step 3 on a log-linear scale (left) and a log-log scale (right), HE-41

The skin is negative, around –3. Permeability values range from 6.4 to 8.8 mD.

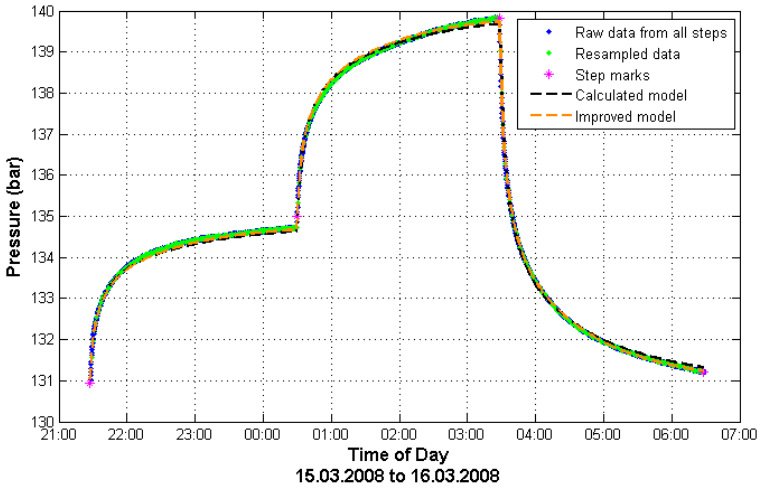

FIGURE 10: Fit between the model and the selected data on a linear scale for all steps, HE-41

3.2 Well HE-42

An injection test with three steps was conducted in vertical well HE-42 on April 12-13, 2008, lasting about 12.5 hours (steps 1 and 2: 3.5 hours each; step 3: 5.5 hours). The pressure gauge was placed at around 1,800 m depth to monitor the pressure changes in the well. The total depth of the well was 3,323 m and the casing reached down to 920 m depth. The three step injection rates were 40, 60 and 25 L/s, respectively (Figure 11) with an initial injection rate of 25 L/s. The figure shows that the pressure response curve of the injection step is not very smooth. The first and second steps show some noisy data with unusual pressure drops which may be the signature of fractures opening in the vicinity of the well. During the analysis, these pressure drops were corrected in the data file. Figure 11 also shows that step 1 started with an initial pressure of 145.19 bar-g and ended with 144.39 bar-g. Each step of the pressure response curve was analysed. With the trial and error method, various models were checked and finally the best model for every step was selected as summarized in Table 4.

TABLE 4: Summary of the model selected For the well test analysis of well HE-42

Reservoir	Homogeneous
Boundary	Constant pressure
Well	Constant skin
Wellbore	Wellbore storage

3.2.1 Modelling of step 1, HE-42

A non-linear regression analysis was performed to find the model parameters that best fit the data gathered. The results from the regression analysis are shown graphically in Figure 12. Figure 13 shows the same data on a log-linear (left) and a log-log scale (right). The plot on the log-log scale shows the derivative of the pressure response multiplied by the time passed since the beginning of the

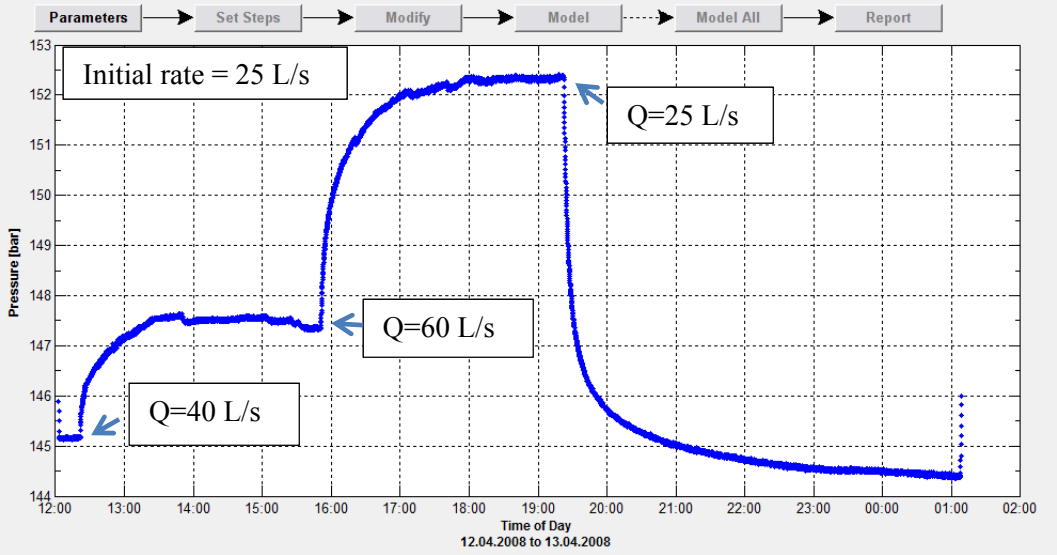

FIGURE 11: Pressure against time at 1750 m depth in well HE-42 during an injection test

step. The model fits the data quite well and can be taken as a representative of the reservoir response to step 1. Based on this model, the calculated different reservoir parameters are presented in Table 5.

3.2.2 Modelling of step 2, HE-42

The results from the regression analysis of step no. 2 are shown graphically in Figure 14 and the same results are shown graphically on a log-linear as well as a log-log scale in Figure 15. The model corresponds quite well to the pressure response of the reservoir. Results for this step are presented in Table 5.

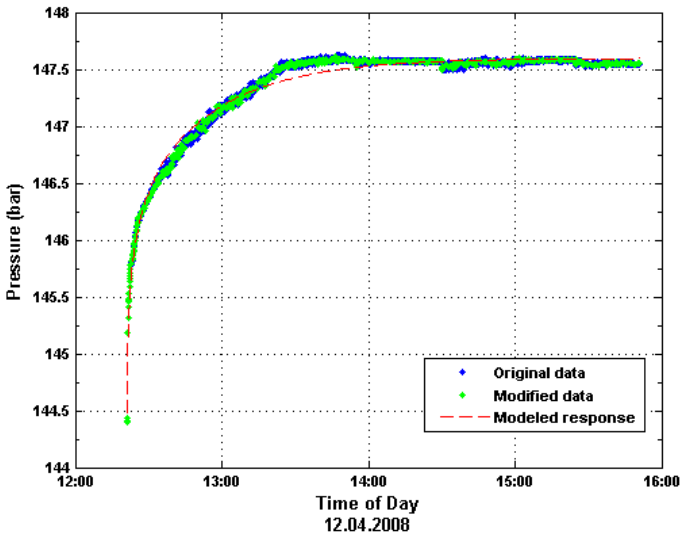

FIGURE 12: Fit between the model and original data for step 1 of well HE-42

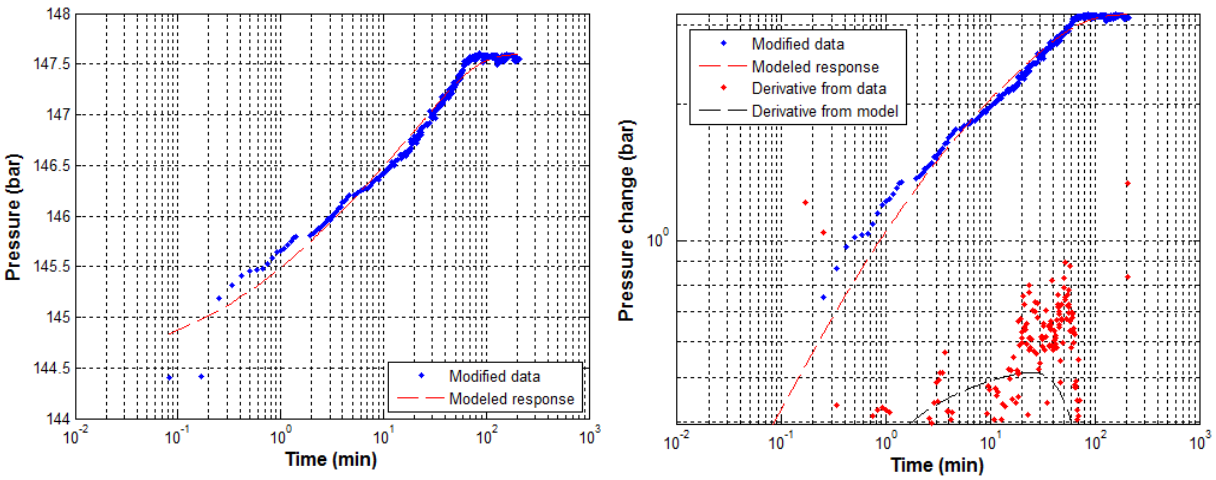

FIGURE 13: Pressure against time showing the fit between the model and the selected data of step no. 1 on a log-linear scale (left) and log- log scale (right), HE-42

TABLE 5: Summary of results from non-linear regression parameter estimates for step 1, step 2, step 3 and all steps jointly, for well HE-42

Parameter name and unit	Step 1		Step 2		Step 3		All steps	
	Values	C_v%	Values	C_v%	Values	C_v%	Values	C_v%
Transmissivity (T) [(m^3/Pa·s)]	2.19×10^{-8}	2.3	1.43×10^{-8}	1.64	4.38×10^{-8}	0.32	3.64×10^{-8}	1.51
Storativity (S) [m^3/(Pa·m^2)]	$4.84 \cdot \times 10^{-8}$	2.10	3.9×10^{-8}	4.41	1.77×10^{-8}	3.3	3.87×10^{-8}	7.16
Radius of investigation (r_e) [m]	72	4.6	65	2.76	285	1.99	151	4.7
Well skin	–3.22		–3.84		–1.3		–1.69	
Wellbore storage (C) [m^3/Pa]	1×10^{-8}	9.76	1.05×10^{-6}	2.6	1.37×10^{-5}	0.34	1.41×10^{-5}	1.52
Injectivity index (II) [(L/s)/bar]	4.75		4		4.4		4.5	
Reservoir thickness [m]	210		170		80		170	
Permeability (k) [m^2]	9.71×10^{-15} (9.7 md)		7.9×10^{-15} (8 mD)		5.3×10^{-14} (53 mD)		2.0×10^{-14} (20 mD)	

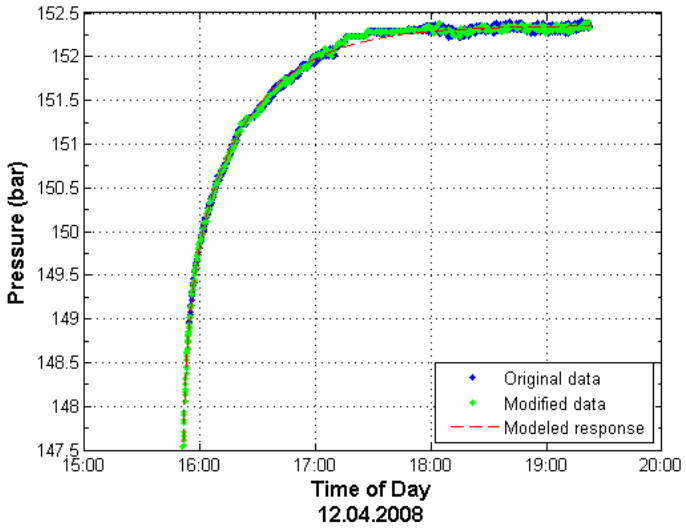

FIGURE 14: Fit between the model and original data for step 2 of well HE-42

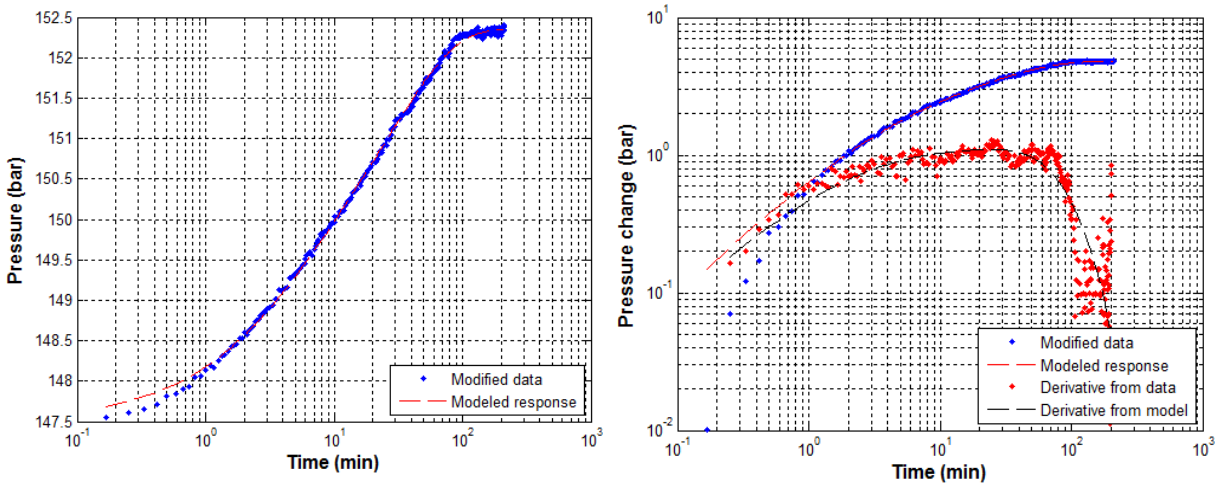

FIGURE 15: Pressure against time showing the fit between the model and the selected data of step 2 on a log-linear scale (left) and a log-log scale (right), HE-42

3.2.3 Modelling of step 3, HE-42

The results from the regression analysis of step 3 are shown graphically in Figure 16 and the same results are shown graphically on a log-linear as well as a log-log scale in Figure 17. The model corresponds quite well with the pressure response of the reservoir. Results for this step are presented in Table 5.

3.2.4 Modelling of all steps, HE-42

The three steps were modelled together, starting with steps 1-3. The results from the regression analysis of the all step model are shown in Figure 18. The graph shows that using the model from step 1 fits best. As stated before, step 1 started with a pressure of 145.19 bar-g and ended with a pressure of 144.39 bar-g. For the all steps model, it was found that no model fitted the data well. But after initial pressure correction, i.e. initial pressure set at 144.39 bar-g, the all steps model fit the data. The results are presented in Table 5.

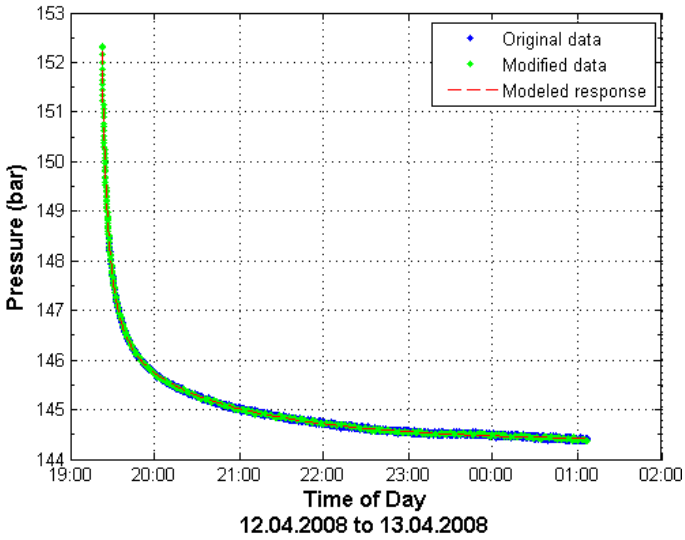

FIGURE 16: Fit between the model and original data for step 3 of well HE-42

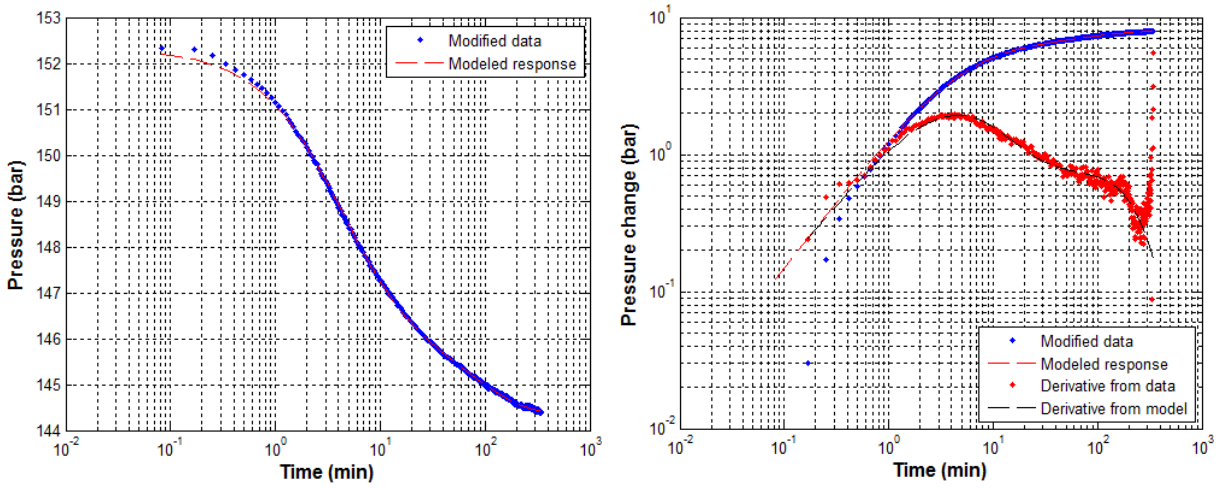

FIGURE 17: Pressure against time showing the fit between the model and the selected data of step no. 3 on a log-linear scale (left) and a log-log scale (right), HE-42

From Table 5 it can be seen that the transmissivity value of step 2 is less than for the other two as well as the all step value. On the other hand, the storativity value of step 3 is less than the other two and the all step value. The skin values of steps 1 and 2 are much closer than step 3 and the all steps value. Permeability values of steps 1 and 2 are close; the step 3 permeability is higher than any other.

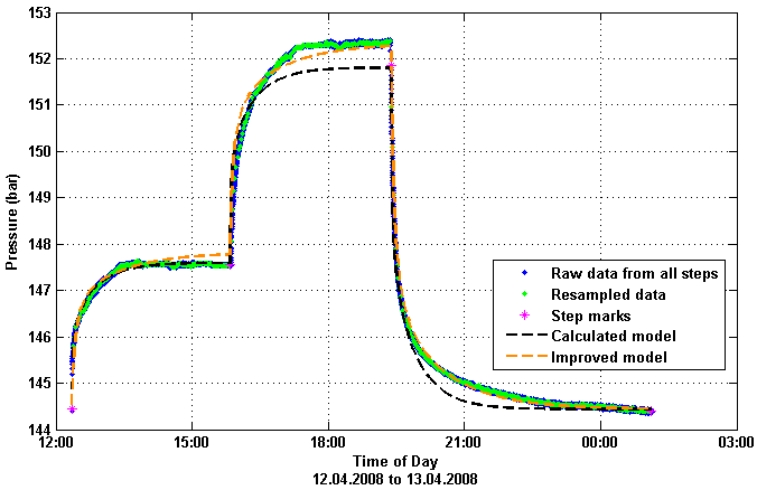

FIGURE 18: Fit between the model and the selected data on a linear scale of all steps of well HE-42

3.3 Well HE-45

A three step injection test was conducted in directional well HE-45 on May 16, 2008 that lasted about 11 hours. The pressure gauge used was placed at around 1,800 m depth to monitor the pressure changes in the well. Total depth of the well was 2,415 m, the casing was placed at 772 m depth and KOP was at 320 m depth. The three step injection rates were 40, 60 and 20 L/s, respectively (Figure 19), with an initial injection rate of 20 L/s. The pressure response curves of the injection steps were very distinct except for step 3 where some instrumental problem occurred. Every step of the pressure response curve was analysed with some modification of step 3. With the trial and error method, various models were checked and finally the best model for each step was selected as summarized in Table 6.

TABLE 6: Summary of the model selected For the well test analysis of well HE-45

Reservoir	Homogeneous
Boundary	Constant pressure
Well	Constant skin
Wellbore	Wellbore storage

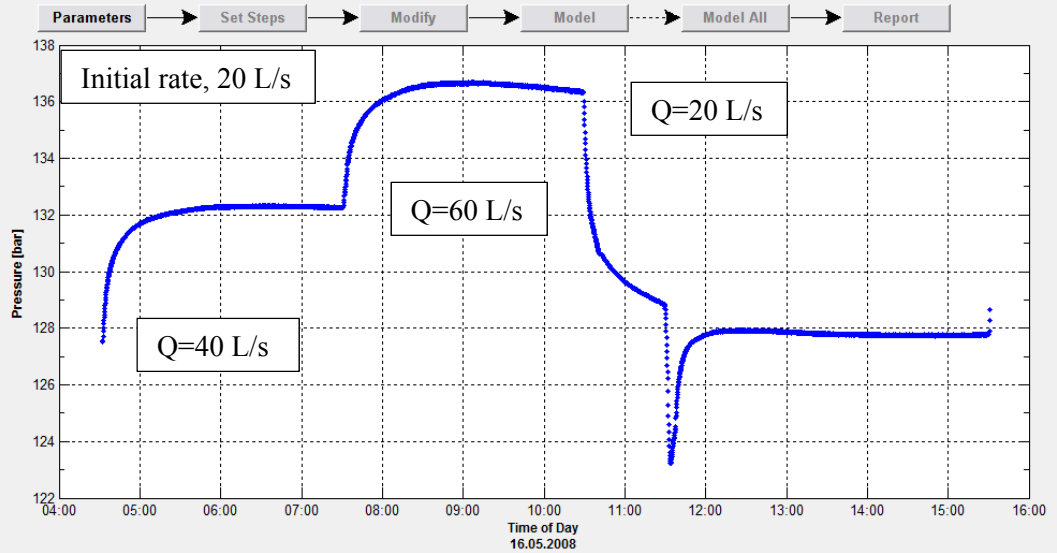

FIGURE 19: Pressure against time at 1800 m depth in well HE-45 during an injection test

3.3.1 Modelling of step 1, HE-45

A nonlinear regression analysis was performed to find the model parameters that best fit the data gathered. The results from the regression analysis are shown graphically in Figure 20. Figure 21 shows the same data on a log-linear (left) and a log-log scale (right). The plot on the log-log scale shows the derivative of the pressure response multiplied by the time passed since the beginning of the step. The model fits the data quite well and can be taken as representative of the reservoir response of step 1. Based on this model, different reservoir parameters were calculated, the results are presented in Table 7.

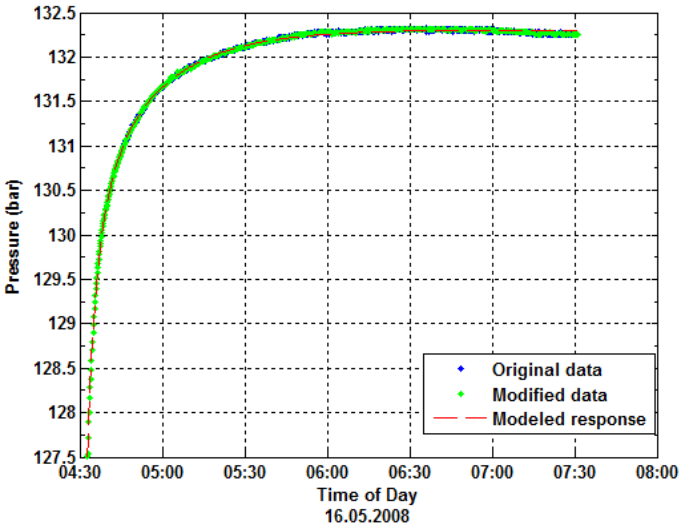

FIGURE 20: Fit between the model and original data for step 1 of well HE-45

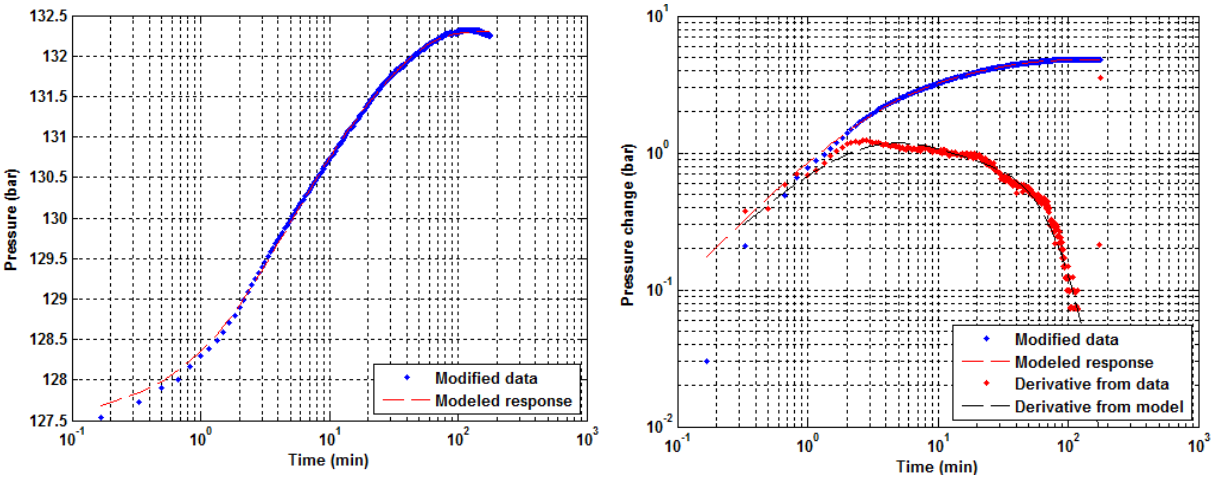

FIGURE 21: Pressure against time showing the fit between the model and the selected data of step 1 on a log-linear scale (left) and log-log scale (right) for well HE-45

3.3.2 Modelling of step 2, HE-45

The results of the regression analysis of step 2 are shown graphically in Figure 22 and the same results are shown graphically on a log-linear as well as a log-log scale in Figure 23. The model corresponds quite well with the pressure response of the reservoir. Results for this step are presented in Table 7.

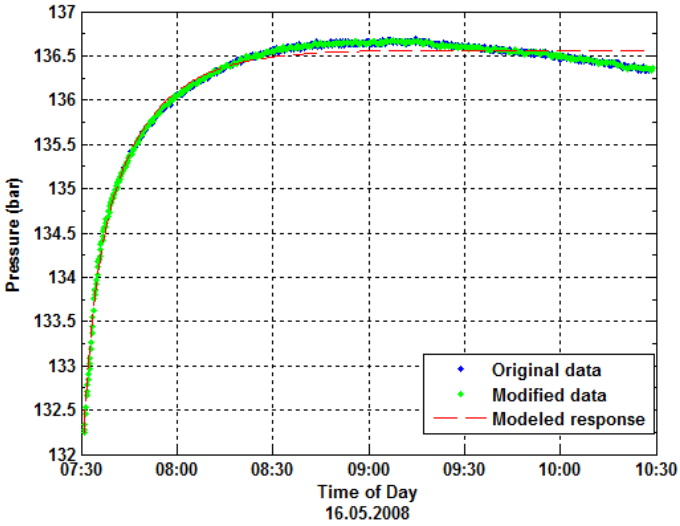

FIGURE 22: Fit between the model and original data for step 2 of well HE-45

3.3.3 Modelling of step 3, HE-45

The results from the regression analysis of step 3 are shown graphically in Figure 24 and the same results are shown graphically on a log-linear as well as a log-log scale in Figure 25. The model corresponds quite well with the pressure response of the reservoir. Results for this step are presented in Table 7. It should be mentioned here that due to the disturbance in the data during the modelling of this step, some corrections were made with WellTester. During correction, some data were excluded and some were added (Figure 24).

TABLE 7: Summary of results from non-linear regression parameter estimates for step 1, step 2, step 3 and all steps jointly, for well HE-45

Parameter name and unit	Step 1		Step 2		Step 3		All steps	
	Values	C_v%	Values	C_v%	Values	C_v%	Values	C_v%
Transmissivity (T) [(m^3/Pa·s)]	2.6×10^{-8}	0.67	2.34×10^{-8}	3.4	3.21×10^{-8}	1.39	3.45×10^{-8}	1.82
Storativity (S) [m^3/(Pa·m^2)]	1.55×10^{-8}	4.2	1.39×10^{-8}	19.38	2.82×10^{-8}	8.38	2.52×10^{-8}	11.76
Radius of investigation (r_e) [m]	112	2.2	90	10.23	150	5.08	183	6.6
Well skin	–2.64		–3.16		–2.46		–1.86	
Wellbore storage (C) [m^3/Pa]	1.05×10^{-8}	0.74	1.57×10^{-6}	2.6	1.23×10^{-5}	2.11	1.18×10^{-5}	4.64
Injectivity index (II) [(L/s)/bar]	4.17		4.6		4.6		4.5	
Reservoir thickness [m]	70		60		130		120	
Permeability (k) [m^2]	3.48×10^{-14} (35 mD)		3.5×10^{-14} (35 mD)		2.3×10^{-14} (23 mD)		2.8×10^{-14} (28 mD)	

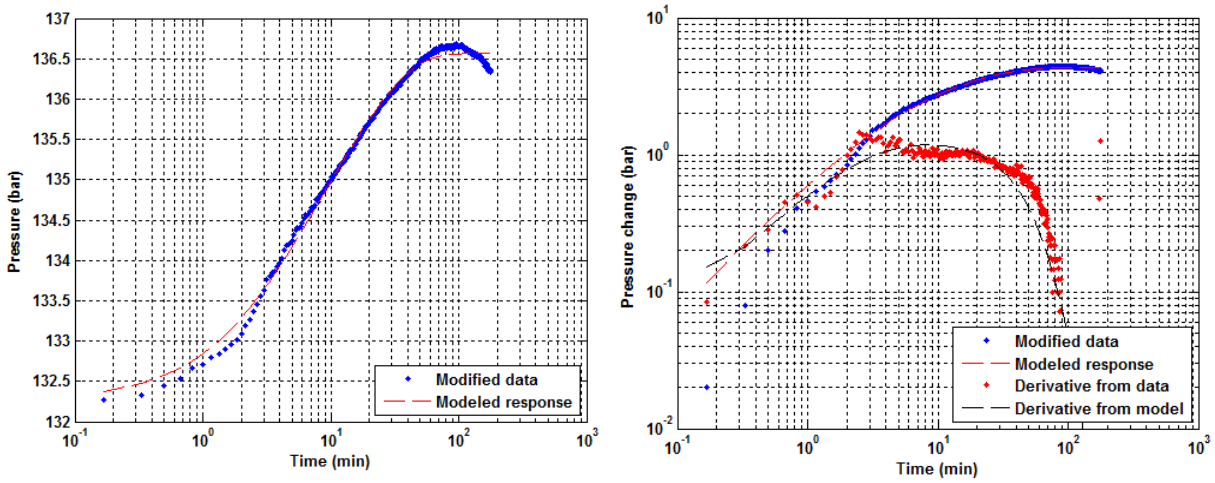

FIGURE 23: Pressure against time showing the fit between the model and the selected data of step 2 on a log-linear scale (left) and a log-log scale (right) for well HE-45

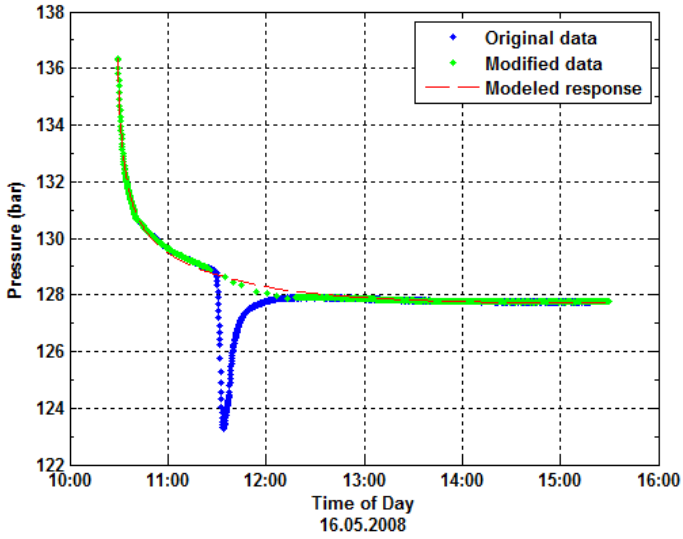

FIGURE 24: Fit between the model and original data for step 3 of well HE-45

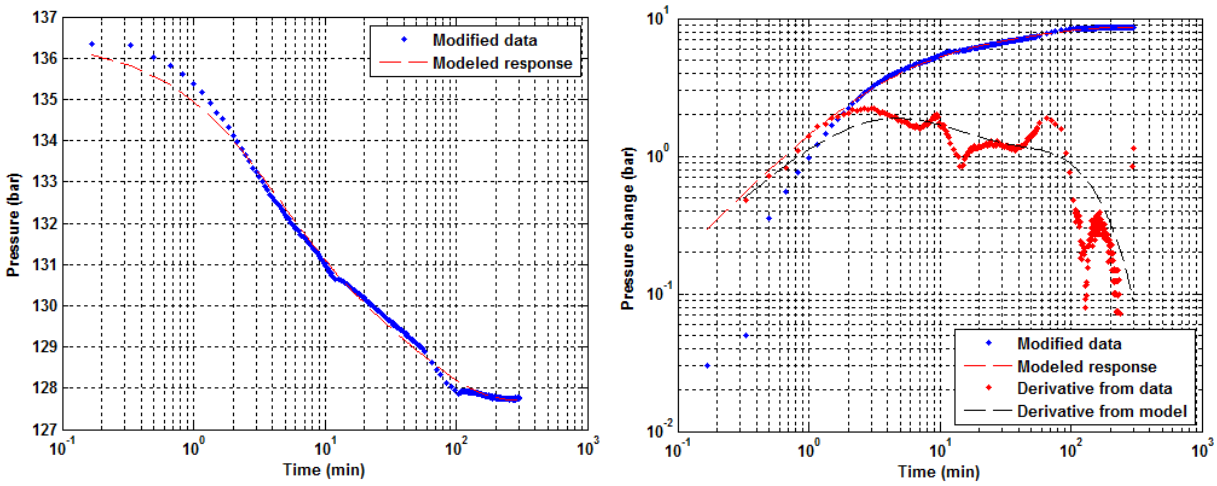

FIGURE 25: Pressure against time showing the fit between the model and the selected data of step 3 on a log-linear scale (left) and log- log scale (right) for well HE-45

3.3.4 Modelling of all steps, HE-45

The three steps were modelled together starting with steps 1-3. The results from the regression analysis of the all steps model are shown in Figure 26. The graph shows that the model from step 1 fits best. The results are presented in Table 7.

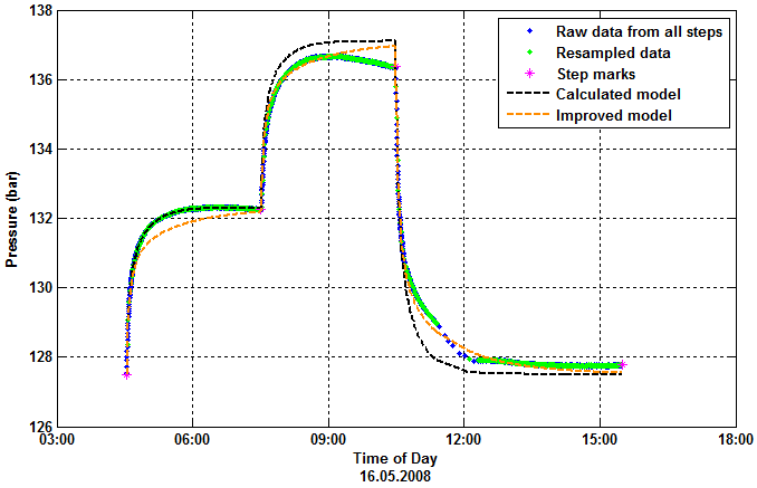

FIGURE 26: Fit between the model and the selected data on linear scale for all steps of well HE-45

Table 7 shows that the transmissivity values for steps 1 and 2 are almost identical whereas the values of step 3 and the all step are much closer. On the other hand, storativity values of steps 1 and 2 are lower than step 3 and the all step values. The skin values are negative and closer for steps 1, 2 and 3 than the all step value. Permeability of steps 1 and 2 are similar; for step 3 and the simulation of all of the steps, the permeability values are closer to each other.

4. RESERVOIR MODELLING WITH LUMPFIT

4.1 General

The main objective of modelling a geothermal system is twofold; one is to simulate pressure changes due to a given production in order to obtain information on the properties of the system and its nature; the other is to obtain information for geothermal resource development and management. The models can then be used to assess the production potential by predicting the future pressure response to different production scenarios. Different techniques are currently being used by the scientific community to model geothermal systems. These approaches utilize a mathematical model that describes a system using mathematical concepts developed to simulate most of the physicochemical and thermodynamic properties of the geothermal system involved. These can be simple analytical models, lumped parameter models or detailed numerical models (Axelsson et al., 2005). The effective lumped parameter model has been successfully used for different geothermal systems in the world. It focuses on the pressure response of the system to production. This method tackles the simulation problem as an inverse problem. It automatically fits analytical response functions of lumped models to the observed data by using a non-linear iterative least-squares technique for estimating the model parameters (Axelsson, 1989).

4.2 Overview of theoretical background

According to Axelsson (1989), a general lumped model consists of a few tanks and flow resistors (Figure 27). The tanks simulate the storage capacity of different parts of the geothermal system. A tank has a storage coefficient (capacitance) κ (kappa) when it responds to a load of liquid mass m with a pressure increase $p = m/\kappa$. The capacitors are connected to resistors (conductors) which simulate the flow resistance in the reservoir controlled by the permeability of the rocks. The mass conductance (inverse of resistance) of a resistor is σ when it transfers $q = \sigma\Delta p$ units of liquid mass per unit time, at the impressed pressure differential Δp (Bödvarsson and Axelsson, 1986). The pressure or water level

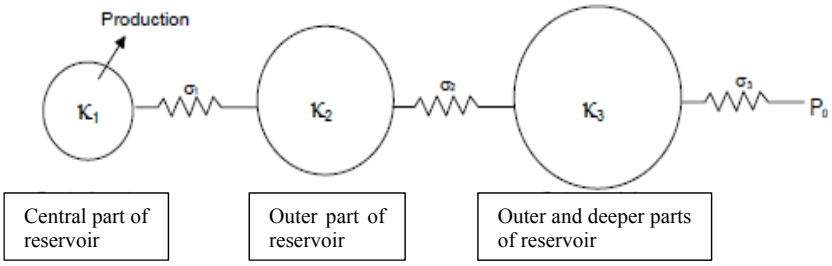

FIGURE 27: A schematic diagram of a lumped parameter model (Axelsson and Gunnlaugsson, 2000)

in the tanks represents the pressure in different parts of the reservoir; production is simulated by water withdrawal from one of the tanks. Figure 27 show a schematic diagram of a three-tank lumped parameter model. The first tank simulates the innermost (production) part of the geothermal reservoir, while the second and the third tanks simulate the outer parts of the system. The third tank is connected by a resistor to a constant pressure source, which supplies recharge to the geothermal system.

The model can either be open or closed. A model is open when the outermost tank is connected by a resistor to an infinitely large imaginary reservoir which maintains a constant pressure. When a model is closed, it is isolated from any external reservoir, i.e. a constant pressure source. So an open model can be considered as an optimistic approach, expecting that equilibrium between production and recharge can be reached during long-term production, causing a stable water level drawdown. In contrast, closed models represent a pessimistic approach where the water level declines continuously during long term production.

Axelsson (1989) presented a system of basic equations describing the behaviour of a general lumped parameter model in matrix form as well as a general solution for the pressure response to variable production. The mass flow from tank *k* to tank *i* is given by:

$$q_{ik=}\,\sigma_{ik}\,(p_k - p_i) \tag{17}$$

while $\sigma_{ik}$is the mass flow conductance of the resistor connecting the tanks and p_k and p_i are the pressures in the tank *k* and *i,* respectively.

The water level, or pressure in the tanks, simulates the water level or pressure in different parts of a geothermal system. Given pressure response, *p*, of a general open lumped model with *N* tanks to constant production, *Q*, (negative if injection) from time $t = 0$ (Bödvarsson and Axelsson, 1986), then, in a general lumped network, the basic equation of the conservation of mass and flow is as follows:

$$\kappa_i \frac{dp_i}{dt} = \sum_{j=1}^{N} q_{ij} - \sigma_i(p_i - p_0) - Q_i \tag{18}$$

$$q_{ij} = \sigma_{ij}(p_j - p_i)$$

Here, *N* is the number of tanks, κ_i is the mass capacitance of the *i*-th tank; Q_i is the production in the *i*-th tank, p_i is the pressure in the *i*-th tank, q_{ij} is the mass flow from the *j*-th tank to the *i*-th tank and σ_{ij} is the flow resistance from the *j*-th tank to the *i*-th tank; in addition, the capacitors are serially connected by up to $N(N–1)/2$ resistors and the conductance of the same element to itself is equal to zero ($\sigma_{ii=0}$).

The solution for the pressure response *p* of a general open lumped model with *N* tanks, to a constant production *Q* since t=0, with initial pressure P_o can be described by Equation19 (Axelsson and Arason, 1992):

$$p(t) = p(t_0) - \sum_{j=1}^{N} Q \frac{A_j}{L_j}[1 - e^{-L_j t}] \quad (19)$$

The pressure response p for a general closed model with N tanks can be described by Equation 20:

$$p(t_i) = p(t_0) - \sum_{j=1}^{N} Q \frac{A_j}{L_j}[1 - e^{-L_j t}] - QBt \quad (20)$$

The coefficients A_j, L_j and B are functions of the storage coefficients of the tanks (κ_j) and the conductance coefficients of the resistors (σ_j) of the model. They can be estimated by using the program LUMPFIT (included in the *ICEBOX* package).

LUMPFIT tackles the simulation problem as an inverse problem and will automatically fit the analytical response functions of lumped models to the observed data by using a nonlinear iterative least-squares technique for estimating the model parameters (Axelsson, 1989) as described previously.

4.3 Lumpfit modelling of OB-1 well

Lumped parameter modelling was used to simulate the pressure response data, taken from an observation well, due to production from two adjacent production wells. One production well was at about 800 m and the other one was at about 1200 m distance from the observation well. To measure the pressure, a pressure bubble gauge was placed about 65 m below the initial water level and approximately 330 m below the surface. First one production well was pumped at about 64 kg/s for 63 days, then shut-in for 30 days. The second production well was pumped at about 47 kg/s for 30 days, then shut-in for 25 days. Finally, both production wells were pumped simultaneously with, on the average, 115 kg/s production for 48 days and shut-in again for 36 days for recovery or pressure build-up. The LUMPFIT model was used to simulate the pressure response of well OB-1. In this model, the pressure response data of the observation well for 232 days of production was used to estimate some reservoir properties and predict future production response for three production scenarios.

Lumpfit modelling is considered a distributed parameter modelling process with a very coarse spatial discretization. There is a methodology described by Axelsson et al. (2005) that is applied to lumped parameter modelling in Iceland. Here, some of the steps are summarized for finding the best parameters for a specific model which could best fit the observed data. First, begin with a one-tank closed model, and then turn to a one-tank open model. After that, a two-tank closed model and a two-tank open model follow. Each model will give suggestions on the initial guesses of the model coefficients for the subsequent more complex model. This should be continued step by step until expanded to a three-tank open model, which is the most complicated model allowed by the program and is sufficient for most systems.

Values for the storage coefficients κ and conductance coefficients σ are obtained by the LUMPFIT program. Some of the properties of the reservoir, e.g. the volume and permeability, were calculated. The parameters for variable sized models are listed in Table 8. During modelling, it was found that two- and three-tank closed and open models yield almost identical matches with the coefficient of determination higher than 99%. After finding the best fitting models, predictions of pressure changes were represented by both an optimistic open version of the model as well as pessimistic predictions by a closed version model for various future production schemes.

From Figure 28, it is clear that some steps of both two- and three-tank open and closed models do not fit perfectly, but the last step, recovery or build up step fits best in all cases.

TABLE 8: Parameters of the best fitting lumped parameter model for OB-1

Parameters	Two tanks		Three tanks	
	Closed	**Open**	**Closed**	**Open**
A_1	7.5×10^{-4}	7.4×10^{-4}	6.8×10^{-4}	6.5×10^{-4}
L_1	6.9×10^{-2}	7.8×10^{-2}	0.101	0.105
A_2		9.3×10^{-5}	1.7×10^{-4}	1.9×10^{-4}
L_2		3.8×10^{-3}	2.6×10^{-2}	3.1×10^{-2}
A_3				5.4×10^{-5}
L_3				7.5×10^{-2}
B	5.9×10^{-5}		4.7×10^{-5}	
κ_1[m·s^2] or [kg/Pa]	1067	1040	970	967
κ_2[m·s^2] or [kg/Pa]	13470	9208	5366	5000
κ_3[m·s^2] or [kg/Pa]			12017	10949
σ_1[m·s] or [(kg/s)/Pa]	7.9×10^{-4}	8.4×10^{-4}	9.2×10^{-4}	9.3×10^{-4}
σ_2[m·s] or [(kg/s)/Pa]		4.5×10^{-4}	1.3×10^{-3}	1.4×10^{-3}
σ_3[m·s] or [(kg/s)/Pa]				1.5×10^{-4}
Root mean square misfit	3.4×10^{-2}	2.9×10^{-2}	2.8×10^{-2}	2.8×10^{-2}
Estimated standard deviation	3.4×10^{-2}	2.9×10^{-2}	2.8×10^{-2}	2.8×10^{-2}
Coefficient of determination	99.3%	99.5%	99.5%	99.5%

By using the parameters, the main reservoir properties of well OB-1were estimated assuming water compressibility c_w to be 6.80 $\times 10^{-10}$ Pa^{-1} at reservoir conditions. The compressibility of the rock matrix c_r was approximately 3.5×10^{-11} Pa^{-1}and the reservoir thickness was estimated at 400 m. The value φ = 0.1 was used for the porosity of the reservoir rock. Storage, in a liquid-dominated geothermal system, could be the result of two types of storage mechanisms. One case is the mobility of a free surface of the reservoir (Equation 21); in the other case, the reservoir is confined and the storage of the reservoir is controlled both by liquid and formation compressibility (Equation 22):

$$S = \varphi / gH \left[\frac{s^2}{m^2}\right] \tag{21}$$

$$S = \frac{\Delta m}{V \Delta p} = \rho_w [\varphi c_w + (1 - \varphi) c_r] \left[\frac{s^2}{m^2}\right] \tag{22}$$

Using the following series of equations, the principal properties and characteristics of the reservoir, such as the volume of the different parts of the system, their areas and permeabilities, could be deduced based on a two-dimensional flow model (Table 9):

$$A_j = \frac{\kappa_j}{Sh} \, [m^2] \, ,$$

$$where \; A = area; h = reservoir \; thickness; \kappa_i = V_i S \, , i = 1,2,3 \ldots . \; ; V = volume$$

$$R_1 = \sqrt{\frac{V_1}{\pi h}}; \; R_2 = \sqrt{\frac{V_1 + V_2}{\pi h}} \; ; \; R_3 = \sqrt{\frac{V_1 + V_2 + V_3}{\pi h}}$$

$$r_1 = \frac{R_1}{2} \; ; \; r_2 = R_1 + \frac{R_2 - R_1}{2}; r_3 = R_2 + \frac{R_3 - R_2}{2}; r_4 = R_3 + \frac{R_3 - R_2}{2}$$

and

$$k_j = \sigma_j \frac{ln\left(\frac{r_{j+1}}{r_j}\right) \nu}{2\pi h} [m^2]; \quad j = 1,2,3 \ldots$$

where υ is the kinematic viscosity of the fluid.

TABLE 9: Reservoir properties of well OB-1 according to lumped parameter models

Model	Properties		First tank	Second tank	Third tank	Total
2-tank closed	Reservoir volume [m^3]	Confined	1.2×10^{10}	1.51×10^{11}		1.6×10^{11}
		Free surface	4.2×10^{7}	5.3×10^{8}		5.7×10^{8}
	Area [m^2]	Confined	3×10^{7}	3.8×10^{8}		4.1×10^{8}
		Free surface	1.1×10^{5}	1.3×10^{6}		1.4×10^{6}
	Permeability [m^2]	Confined	8.5×10^{-14} (85 mD)			
2-tank open	Reservoir volume [m^3]	Confined	1.2×10^{10}	1.03×10^{11}		1.2×10^{11}
		Free surface	4.1×10^{7}	3.6×10^{8}		4.02×10^{8}
	Area [m^2]	Confined	2.9×10^{7}	2.6×10^{8}		2.9×10^{8}
		Free surface	1.02×10^{5}	9.02×10^{5}		1.0×10^{6}
	Permeability [m^2]	Confined	8.2×10^{-14} (82 mD)	2.2×10^{-14} (22 mD)		
3-tank closed	Reservoir volume [m^3]	Confined	1.1×10^{10}	6×10^{10}	1.3×10^{11}	2.1×10^{11}
		Free surface	3.8×10^{7}	2.1×10^{8}	4.7×10^{8}	7.2×10^{8}
	Area [m^2]	Confined	2.7×10^{7}	1.5×10^{8}	3.4×10^{8}	5.13×10^{8}
		Free surface	9.5×10^{4}	5.3×10^{5}	1.2×10^{6}	1.8×10^{6}
	Permeability [m^2]	Confined	8×10^{-14} (80 mD)	6.1×10^{-14} (61 mD)		
3-tank open	Reservoir volume [m^3]	Confined	1.2×10^{10}	5.6×10^{10}	1.2×10^{11}	1.9×10^{11}
		Free surface	3.8×10^{7}	1.9×10^{8}	4.3×10^{8}	6.6×10^{8}
	Area [m^2]	Confined	2.7×10^{7}	1.4×10^{8}	3.1×10^{8}	4.7×10^{8}
		Free surface	9.5×10^{4}	4.9×10^{5}	1.1×10^{6}	1.7×10^{6}
	Permeability [m^2]	Confined	7.9×10^{-14} (80 mD)	6.5×10^{-14} (65 mD)	4.3×10^{-15} (4 mD)	

4.4 Interpretation and prediction

Two-tank open and closed models, as well as three-tank open and closed models, were used to simulate the pressure data individually. The results of the two- and three-tank open and closed models are shown in Figure 28. The parameters of these two models are presented in Table 8 for comparison. The coefficients of determination reveal that the two- and three-tank open and closed models are regarded as the most appropriate models for the presently studied well. Consequently, we can use the parameters of the two individual models to estimate the reservoir properties, i.e. permeability and reservoir volume and area. The surface area for the two-tank closed and open models is 410 km^2 and 290 km^2, respectively, whereas it is 513 km^2 and 470 km^2 for the three-tank closed and open models, respectively.

On the other hand, the permeability value was about 85 mD for the two-tank closed model, 82 mD for the first tank, and 22 mD for the second tank of the two-tank open model. The permeability was 80 and 61 mD for the first and second tanks of the three-tanks closed model, respectively, whereas it was 80, 65 and 4 mD for the first, second and third tanks, respectively, of the three-tanks open model. The first and second tanks of both two- and three-tanks closed and open models had higher permeability. It is also clear that the first tank had higher permeability than the second. It indicated good fluid transport conditions between the inner and outer tanks. It also revealed that the inner tank had good recharge conditions.

The predictions and simulations were made based on the data available. The amount (of the data sample) and duration (time length) of the data definitely affected the reliability of the simulations as

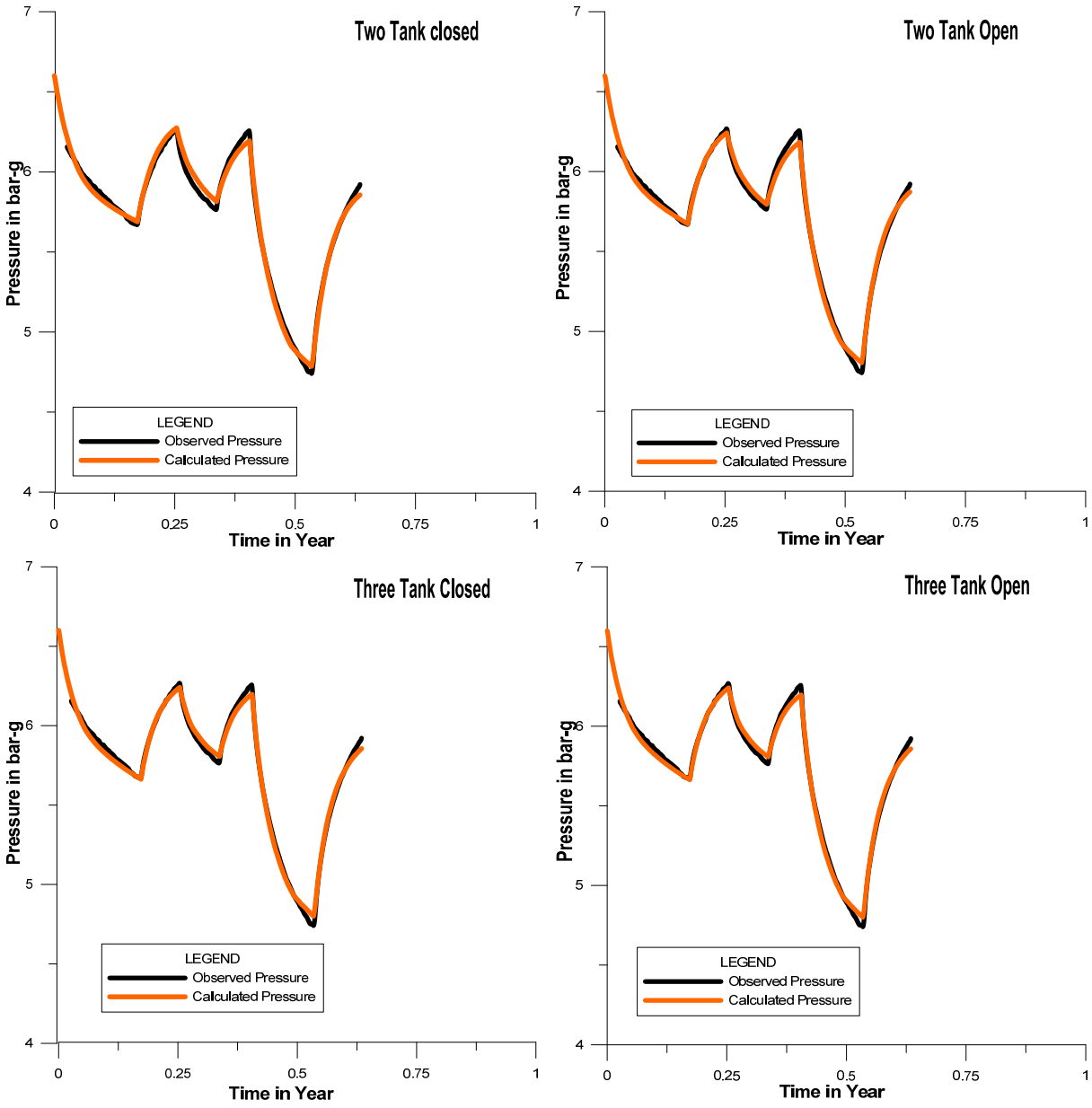

FIGURE 28: Observed and simulated pressure response data for well OB-1 by two- and three-tank closed and open models

well as the future production response. No accurate future predictions can be done until enough production data has been collected for a reliable simulation.

In order to assess the production potential and pressure variations in the future, both open and closed models were used to predict the pressure changes for three different production scenarios; these were selected by assuming a production of 80, 120 and 180 kg/s on average. A ten years prediction period was chosen. The predicted pressure drops for these three scenarios are shown in Figures 29 and 30.

Based on the prediction results shown in Figure 29, the open model indicates that the reservoir could sustain a production rate of 180 kg/s for 10 years with an average pressure drop of maximum 7.5 bar for the three-tank open model, but about 6 bar for the two-tank open model. It was also noticeable that in both open models, the pressure stabilized within two and a half years and three and a half years, respectively. This shows that withdrawal from the inner reservoir could be kept at equilibrium with recharge coming from the outer area, according to the open model. It also indicates that the

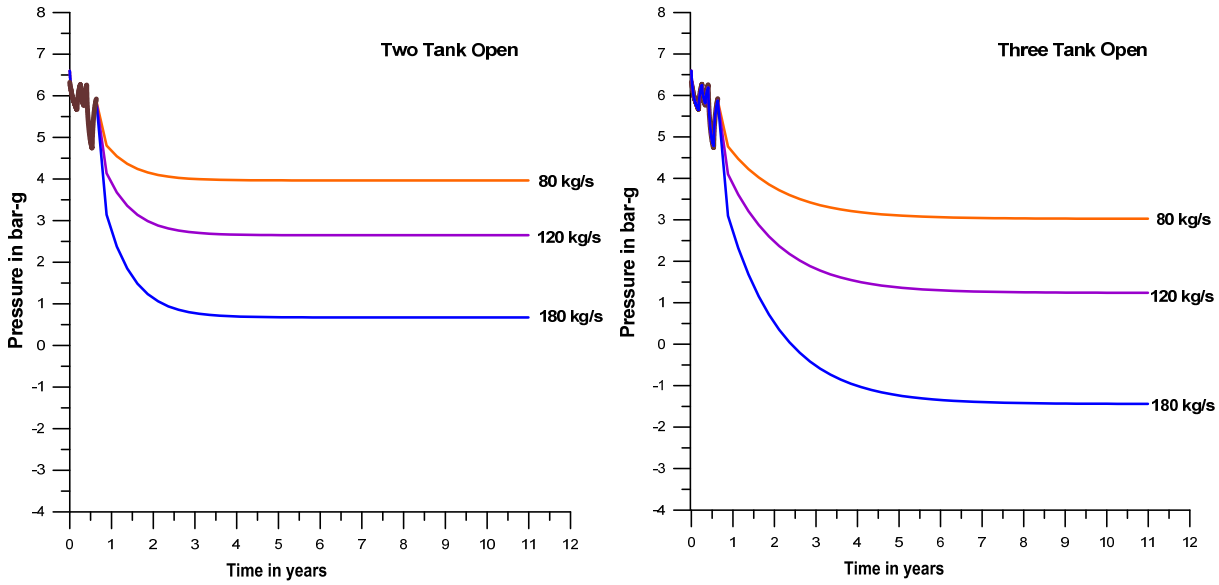

FIGURE 29: The predicted pressure response to 80, 120 and 180 kg/s future production; the prediction of two- and three-tank open models

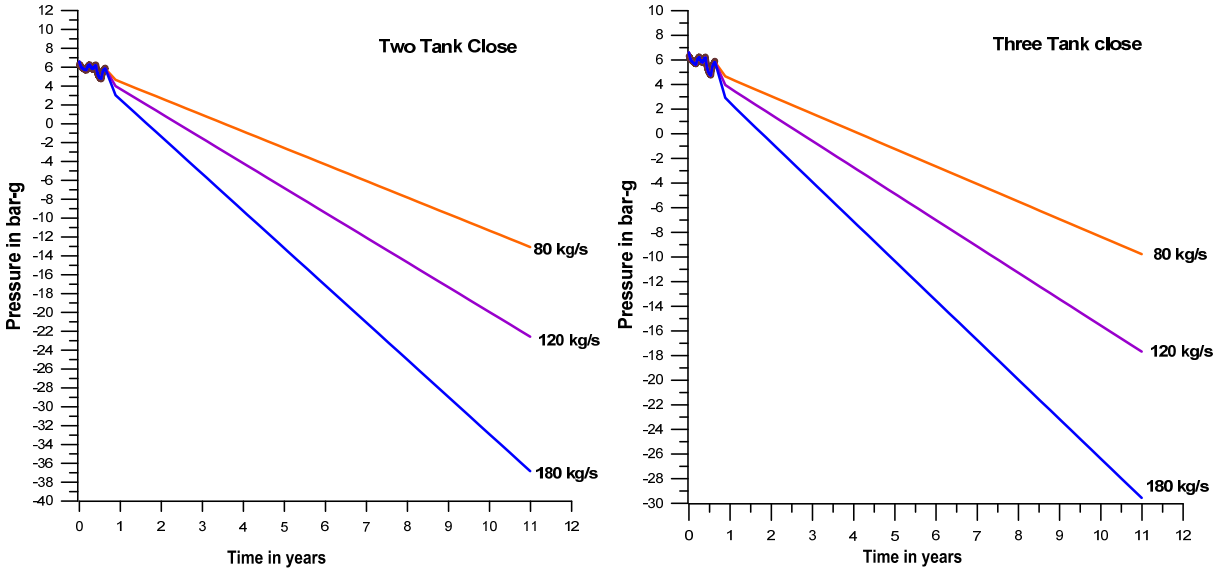

FIGURE 30: The predicted pressure response to 80, 120 and 180 kg/s future production; the prediction of two- and three-tank closed models

surrounding recharge area could supply sufficient fluid to maintain a nearly stable pressure. From the graphical presentation (Figure 30), it can also be seen that in the two- and three-tank closed models, the future pressure response curve falls continuously. The closed models predict that the pressure will drop continuously with a pressure drop of more than 38 bar for a two-tank closed model and 33 bar for a three-tank closed model, over a 10 year period of 180 kg/s production.

5. DISCUSSION OF THE RESULTS AND CONCLUSIONS

The WellTester software was used to calculate reservoir parameters for an injection step analysis and the LUMPFIT software was used to calculate some reservoir properties as well as for predicting the

future pressure response due to production, using data from an interference test conducted in a nearby observation well. These two programs enable the use of different pressure models to try to fit raw data and to calculate various reservoir parameters. In WellTester these parameters include transmissivity, storativity, wellbore storage, skin effect, reservoir volume and permeability; some of these can also be calculated by LUMPFIT. The output plots of the WellTester and LUMPFIT programs are shown in Figures 3-26 and 26-30, respectively. The calculated parameters of both programs are given in Tables 3, 5, 7, 8, and 9. Calculated parameters were close to the values generally found in Iceland.

Transmissivity is the major parameter which describes or characterizes the ability of a reservoir to transmit fluid. Largely, it is affected by the pressure gradient between the well and the boundary of the reservoir. The studied area consists mainly of hyaloclastite formations (sub-glacial) which are characterized by uniform fissures and fractures. In Iceland, this formation works as a main aquifer of geothermal systems. Júlíusson et al. (2008) stated that for Icelandic geothermal reservoirs, the transmissivity T is on the order of 10^{-8} $m^3/(Pa{\cdot}s)$. The results for the transmissivity of the studied wells was 2.0×10^{-8} $m^3/(Pa{\cdot}s)$ for HE-41, 3.6×10^{-8} $m^3/(Pa{\cdot}s)$ for HE-42 and 3.5×10^{-8} $m^3/(Pa{\cdot}s)$ for HE-45. All the transmissivity values were similar and similar to expected values for Icelandic geothermal wells.

How fast the pressure front can travel within the reservoir depends on the storativity and the transmissivity of that reservoir. Again, storativity depends on fluid compressibility. So it varies greatly between reservoir types, i.e. liquid-dominated vs. two-phase or dry steam (Grant et al., 1982). Common values for liquid-dominated geothermal reservoirs are around 10^{-8} $m^3/(Pa{\cdot}m^2)$ while two-phase reservoirs might have values on the order of 10^{-5} $m^3/(Pa{\cdot}m^2)$. The results for HE-41 gave a storativity value of $4.9{\times}10^{-8}$ $m^3/(Pa{\cdot}m^2)$, while the values for HE-42 were $3.9{\times}10^{-8} m^3/(Pa{\cdot}m^2)$ and $2.5{\times}10^{-8}$ $m^3/(Pa{\cdot}m^2)$ for HE-45. Therefore, it can be said that this is a liquid-dominated geothermal reservoir.

For damaged wells, the skin factor is positive and for stimulated wells it is negative. The skin factor for geothermal wells in Iceland is commonly negative, around –1 to –2, although values may range from about –5 to 20. In all of the studied wells, the skin factor values were within the range of –3.2 and –1.69; the values were negative which means that the wells are stimulated.

The injectivity index (*II*) is often used as a rough estimate of the connectivity of a well to the surrounding reservoir. The results for HE-41, 42 and 45 were in the range of 4–4.5 (L/s)/bar. It was also revealed that the results for the injectivity index were quite consistent for all of the studied wells. Reservoir thickness, estimated by WellTester, was 290 m for HE-41, 168 m for HE-42 and 116 m for HE-45, which is probably an underestimate. Further investigations are needed for accurate estimates of the reservoir thickness.

Permeability can vary by a few orders of magnitude but common values from injection testing in Icelandic geothermal reservoirs are on the order of 10–100 mD. The results for the studied wells in Hellisheidi were 7, 20 and 28 mD, respectively.

Regarding the various other parameters given in Tables 3, 5 and 7, it can be seen that the values found for different parameters were usually typical for values found in Iceland. Also note that more realistic values were found when the steps were fitted separately. When all the data were modelled together, the values of the parameters changed a little bit. It can be difficult to fit all three steps in the same model.

The coefficient of determination of the Lumpfit parameters indicates that the parameters are well determined by the model from the data. In our study, it was found that for all models the coefficients of determination are over 99%. For a constant production rate of three production scenarios for duration of 10 years of two- and three-tank open models, the reservoir pressure of the system declined sharply at early times and then reached a constant value at late times which indicates a good fluid

conduit between the inner and outer tanks. On the other hand, for the two- and three-tank closed models, the pressure declines continuously up to 38 and 33 bar for a constant production of 180 kg/s,, equivalent to a water level decline of approximately 380 and 330 m, respectively.

Results of the two-tank and three-tank closed and open model simulations did not exhibit any significant differences; further information and detailed analyses are required to identify the most appropriate model for the system/well studied. The geological and geophysical conditions in the area should also be considered when choosing the most appropriate model.

ACKNOWLEDGEMENTS

I would like to thank the government of Iceland and the United Nations University for supporting me in accomplishing this training programme. I would sincerely like to express my heartfelt gratitude to Dr. Ingvar B. Fridleifsson, Director, and Mr. Lúdvík S. Georgsson, Deputy Director, for giving me the opportunity to attend the UNU Geothermal Training Programme and for their moral support and help throughout the whole training period. Sincere thanks go to my supervisors, Mr. Páll Jónsson and Dr. Svanbjörg H. Haraldsdóttir, for providing me with patient guidance, advice, shared knowledge and experience. Also, special thanks go to Dr. Gudni Axelsson for providing me with excellent help and assistance. I appreciate miscellaneous help from Ms. Thórhildur Ísberg, Ms. Dorthe H. Holm, Mr. Markús A.G. Wilde and Mr. Ingimar G. Haraldsson during the training. I also want to thank all teachers in Iceland for providing me with very special knowledge, and the employees of ISOR and Orkustofnun for their sincere help in numerous ways.

I would like to acknowledge the Government of Bangladesh, through the Ministry of Energy and Mineral Resources, Geological Survey of Bangladesh for giving permission to attend the six months programme in Iceland.

I am grateful to the reservoir engineering group, especially Vincent and Liu, along with the other UNU Fellows for their support over the last six months.

Finally, I am grateful to almighty Allaha for his grace and protection throughout my stay in Iceland and for keeping my beloved family safe.

REFERENCES

Árnason, K., Eysteinsson, H., and Hersir, G.P., 2010: Joint 1D inversion of TEM and MT data and 3D inversion of MT data in the Hengill area, SW Iceland. *Geothermics, 39,* 13-34.

Axelsson, G., 1989: Simulation of pressure response data from geothermal reservoir by lumped parameter models. *Proceedings of the 14th Workshop on Geothermal Reservoir Engineering, Stanford University, California*, 257-163.

Axelsson, G., and Arason, Th., 1992: *LUMPFIT, automated simulation of pressure changes in hydrogeological reservoirs. User's guide version 3.1.*Orkustofnun, Reykjavík, Iceland, 32 pp.

Axelsson, G., Björnsson, G., and Quijano, J., 2005: Reliability of lumped parameter modelling of pressure changes in geothermal reservoirs. *Proceedings of the World Geothermal Congress 2005, Antalya, Turkey,* CD, 8 pp.

Axelsson, G., and Gunnlaugsson, E., 2000: Long-term monitoring of high- and low-enthalpy fields under exploitation. *World Geothermal Congress 2000, Pre-congress Course, Kokonoe, Japan,* 226 pp.

Bödvarsson, G., and Axelsson, G., 1986*: The analytical framework of the simulation of liquid reservoir response functions by lumped element models*. Oregon State University, unpublished report, 71 pp.

Earlougher, R.C., Jr. 1977: *Advances in well test analysis*. SPE, NY, Dallas.

Fridleifsson, G.Ó., 1983: *The geology and the alteration history of the Geitafell central volcano, southeast Iceland.* University of Edinburgh, Grant Institute of Geology, Faculty of Science, PhD thesis, 371 pp.

Geirsson, H., Árnadóttir, Th., Hreinsdóttir, S., Decriem, J., LaFemina, P.C., Jónsson, S., Bennett, R.A., Metzger, S., Holland, A., Sturkell, E., Villemin, T., Völksen, C., Sigmundsson, F., Einarsson, P., Roberts, M.J., and Sveinbjörnsson, H., 2010: Overview of results from continuous GPS observations in Iceland from 1995 to 2010. *Jökull, 60*, 3-22.

Grant, M.A., Donaldson, I.G., and Bixley, P.F., 1982: *Geothermal reservoir engineering*. Academic Press Ltd., NY, 369 pp.

Horne, R.N, 1995: *Modern well test analysis – a computer-aided approach* (2nd ed.). Petroway, Inc., Palo Alto, CA, 257 pp.

Jakobsson, S.P., 1972: Chemistry and distribution pattern of recent basaltic rocks in Iceland. *Lithos, 5,* 365-386.

Júlíusson, E., Grétarsson, G.J., and Jónsson, P., 2008: *WellTester 1.0b user´s guide.* ÍSOR – Iceland GeoSurvey, Reykjavík, report ÍSOR-2008/063, 27 pp.

Saemundsson, K., 1978: Fissure swarms and central volcanoes of the neovolcanic zones of Iceland. *Geol. J., Spec. Issue, 10,* 415-432.